

Supporting Information for

A novel paradigm for fabricating highly uniform nanowire arrays using residual stress-induced patterning

ZnO NWs fabricated on Zn seed layer sputtered on Si substrate

Comparative experiments were conducted using Zn seed layers chemically grown on Si substrates. NW arrays were grown on 50, 100 and 300 nm wide patterns from solution of 20 mmol/L concentration at 96 °C for 20 minutes. It was found that the number of the ZnO NWs could be controlled by varying the opening sizes (Fig. S1). This indicated that our fabrication method was able to produce both single ZnO NWs and NW clusters.

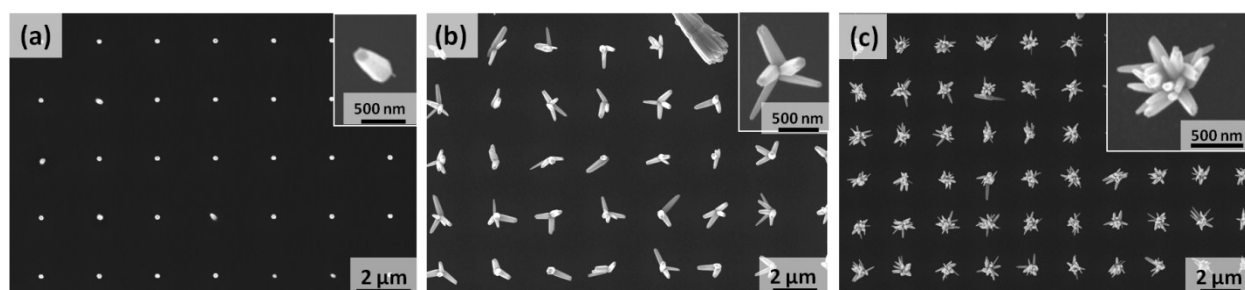
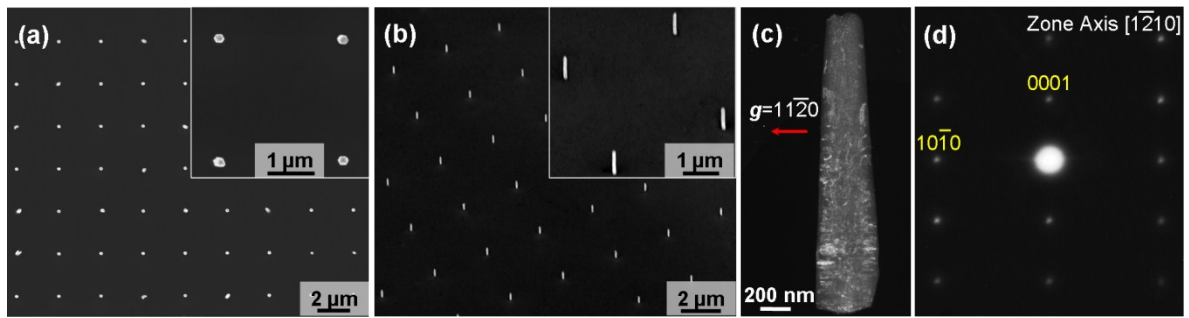


Fig. S1 SEM images of ZnO NW grown in 20 mmol/L concentrated solution, on 2-D patterned 50-80 nm PS film mask-covered Zn seed layer on Si substrates. The opening diameters in (a), (b) and (c) are 50, 100 and 300 nm.

Universality - on arbitrary substrates

The epitaxial growth of ZnO NW from ZnO substrates resulted in very well aligned single NW array, however the non-conductive ZnO substrate cannot be integrated into optoelectronic devices, unless highly doped, used which would then increase the cost enormously. Wide application, especially the integration in electronics, favours the use of arbitrary substrates, especially Si and ITO coated glass, which are usually used in photovoltaics and light emitting diodes.



1
 2 **Fig. S2** Morphology and crystallinity of ZnO NW array grown on textured ZnO coated Si substrate
 3 with patterned PS film as mask, from 20 mmol/L concentrated solution for 120 minutes. (a) plane
 4 view SEM image; (b) the corresponding 45°tilt view images. (c) Weak beam dark field TEM
 5 image; (d) TEM diffraction pattern taken on zone axis [1-210], with two typical diffraction spots
 6 labelled.

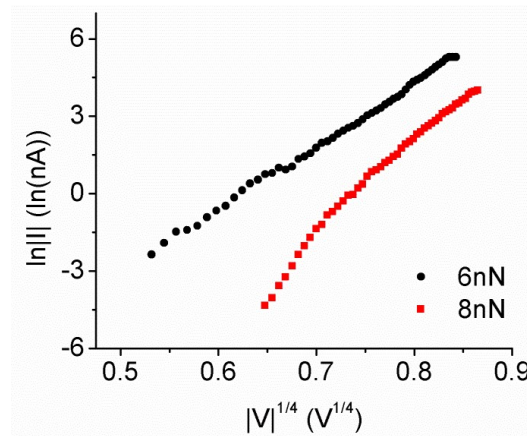
7 Using textured ZnO as a seed layer on top of Si substrate, we successfully made the vertically
 8 well-aligned ZnO NW array, as shown in Fig. S2. They have very similar morphology to the NWs
 9 grown on ZnO substrates under identical conditions, while they are slightly thinner and not as
 10 perfectly vertical as those on ZnO substrates. The length and top diameter of NWs grown from 100
 11 nm wide openings are 1.2 μm and 180 nm, respectively. It has been noticed that this diameter is
 12 smaller than the diameter of the NWs grown from the same sized openings on sc-ZnO substrate,
 13 which is 560 nm at the NW bottom and 211 nm at the NW top. This is presumably due to the
 14 difference in the crystal size and orientation of the deposited ZnO layer from the sc-ZnO substrate.
 15 This comparison indicates that the crystallinity of the seed layer played a key role in determining
 16 the morphology of the patterned ZnO NW array, especially the orientation and the number of NWs
 17 in a single opening. On the polycrystal seed layer, most of the NWs grown in the 50 nm wide
 18 circular holes were single NWs in each opening, while multiple NWs grew in larger sizes openings
 19 (see Fig. S1).

20 The crystal structure of the as-produced NW array on Si substrate was examined by TEM. The
 21 TEM diffraction patterns (Fig. 3e) showed that the NWs grown on Si substrate are also single
 22 crystal. The weak beam dark field image revealed the presence of some structural defects inside
 23 the NWs grown on ZnO/Cr/Si, similar to those grown on ZnO substrates.

24 The equally good results for ZnO NWs grown from Si substrate coated with a textured ZnO layer
 25 indicates the universal paradigm has good compatibility with a wide range of materials, and
 26 particularly will be beneficial for the integration of NWs in electronic devices, such as
 27 photovoltaics and light emitting diodes, which usually use Si and ITO coated glass.

1 **Dependence of current on bias**

2 Schottky contact presumably existed between ZnO nanowire and the AFM tip. To verify the I-V
 3 relationship,¹ we plug in the equation with the data in I-V curves (Fig. 5d) measured under 6 and 8
 4 nN vertical compression force, and obtained the linear plot shown in Fig. S3. It can be clearly seen
 5 that the I-V relationship well fits the following equation: $\ln |I| \propto |V|^{1/4}$.



6
 7 **Fig. S3** Plots of $\ln|I|$ as a function of $|V|^{1/4}$, by using the data from the negative biased region in
 8 Fig. 5d.

9 **Statistical data of multiple cAFM piezoelectric experiment results of vertical manipulation of**
 10 **single as-grown NW**

11 In order to investigate the repeatability and reliability of the cAFM piezoelectric experiments,
 12 multiple experiments (20-30 times) were performed with the cAFM cantilever tip pressing at
 13 positions of “1” (center of the NW), “2”, “3”, and “4”, respectively. The height and diameter of the
 14 NWs employed in the experiments are 3.2 μm and 250 nm, respectively. The STD averaged data
 15 for different positions at 80 nm deflection were summarized in Table S1.

16 **Table S1** Statistical data of multiple cAFM piezoelectric experiment results of vertical pressing
 17 single NW by an AFM tip:

Position	1	2	3	4
Distance from center (NW $\Phi=250\text{nm}$, height=3.2 μm)	0	38	76	114
Current (pA)	$0.2 \pm$	$56 \pm$	$95 \pm$	$136 \pm$
(average \pm standard deviation)	0.1	15	32	38

1 Calculations of the piezoelectric voltage

2 A simple calculation was employed to estimate the piezoelectric voltage when the cAFM tip was
3 positioned “1” (center of the top surface of the ZnO nanowire as shown in Fig. 5b), using the
4 classical model of piezoelectricity generation. The piezoelectric field E is defined as

$$5 \quad E = \frac{\varepsilon}{d} \quad (1)$$

6 where ε is the stress and d is piezoelectric coefficient, respectively. Assuming the original length
7 of the ZnO NW is L , and under the cAFM tip pressing the NW is shortened ΔL along the c -axis of
8 the NW, then the piezoelectric potential is generated as

$$9 \quad V = \int_0^{\Delta L} E dy = \int_0^{\Delta L} \frac{\varepsilon}{d} dy = \int_0^{\Delta L} \frac{y}{dL} dy = \frac{\Delta L^2}{2Ld} \quad (2)$$

10 When a single ZnO NW with diameter of D is under the external force F along the c -axis from
11 the cAFM tip pressing at the center of the NW, the deformation of the NW (i.e., shortened length
12 ΔL) is ,

$$13 \quad \Delta L = \frac{F \cdot L}{Y \cdot \left(\frac{3\sqrt{3}}{8} D^2\right)} \quad (3)$$

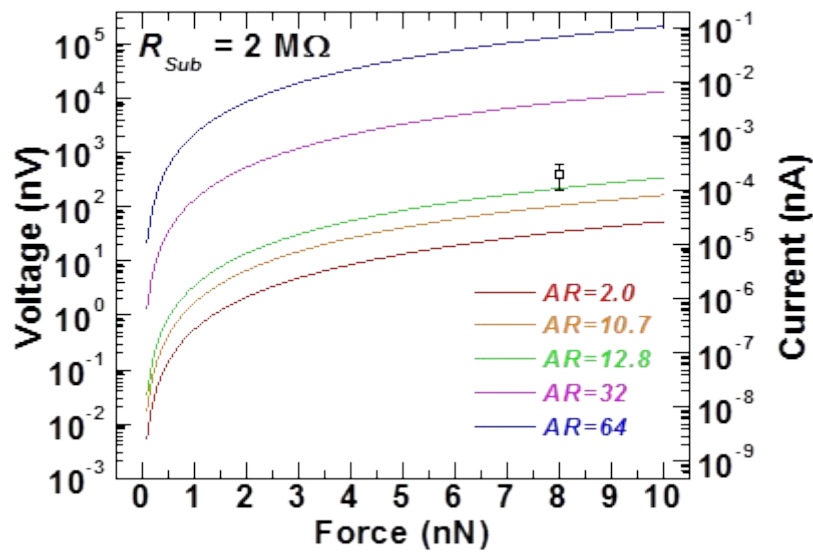
14 where Y is the Young's modulus of ZnO and $\left(\frac{3\sqrt{3}}{8} D^2\right)$ is the area of the hexagonal cross-section
15 of the ZnO NW.

16 Employ Equation (3) into Equation (2), the relation between piezoelectric voltage and the
17 external force is obtained as

$$18 \quad V = \frac{\Delta L^2}{2Ld} = \frac{32L \cdot F^2}{27Y^2 D^4 \cdot d} \quad (4)$$

19 For convenience sake, aspect ratio (AR) is used for plotting, which is defined as L/D . With the
20 approximate values of ZnO c -axis piezoelectric constant $d \approx 12.4$ pm/V and Young's modulus $Y \approx$
21 150 GPa^{2,3} the relation between the piezoelectric voltage and the external force is shown in Fig. S4
22 based on equation (4) of ZnO NWs with different AR. Apparently, the piezoelectric potential

1 generated under constant external force increased with the AR and consequently the deflection of
2 the NWs..



3
4 **Fig. S4** Calculation of the piezoelectric potential and externally applied force along the c-axis from
5 the cAFM tip on the top center of the ZnO NW.

6 Using the spring constant of the cAFM cantilever is 0.1 N/m, the deflection of the cantilever can
7 be converted to the applied force. Based on the I-V characteristics when the cAFM tip is placing
8 on the ZnO substrate (position “0”) as shown in Fig. 4(b) in the paper, the external resistance in the
9 loop is approximately estimated as 2 MΩ. The piezoelectric current in the experiments can be
10 converted as piezoelectric voltage using the external resistance. The experimentally measured
11 current at position 1 summarized in Table S1 are shown in Fig. S4 with STD average and error bar,
12 which is approximately in line with the calculated value. It need to be aware that in this simple
13 calculation the ZnO NW is deformed “vertically” when the cAFM tip is pressing at position 1.

14
15
16
17
18

1 References

- 1 W. Han, Y. Zhou, Y. Zhang, C.Y. Chen, L. Lin, X. Wang, S. Wang and Z. L. Wang, *ACS Nano*, 2012, **6**, 3760.
- 2 J. A. Christman, H. Maiwa, S. H. Kim, A. I. Kingon and R. J. Nemanich, *Appl. Phys. Lett.*, 1998, **73**, 3851.
- 3 M. H. Zhao, Z. L. Wang and S. X. Mao, *Nano Lett.*, 2004, **4**, 587.